Impact of Coulomb Scattering on the Ultrafast Gain Recovery in InGaAs Quantum Dots

J. Gomis-Bresco, S. Dommers, V. V. Temnov, and U. Woggon*
Institut für Optik und Atomare Physik, Technische Universität Berlin, 10623 Berlin, Germany

M. Laemmlin and D. Bimberg
Institut für Festkörperphysik, Technische Universität Berlin, 10623 Berlin, Germany

E. Malic, M. Richter, E. Schöll, and A. Knorr
Institut für Theoretische Physik, Technische Universität Berlin, 10623 Berlin, Germany
(Received 6 June 2008; published 16 December 2008)

The application of quantum dot (QD) semiconductor optical amplifiers (SOAs) in above 100-Gbit Ethernet networks demands an ultrafast gain recovery on time scales similar to that of the input pulse ~100 GHz repetition frequency. Microscopic scattering processes have to act at shortest possible time scales and mechanisms speeding up the Coulomb scattering have to be explored, controlled, and exploited. We present a microscopic description of the gain recovery by coupled polarization- and population dynamics in a thermal nonequilibrium situation going beyond rate-equation models and discuss the limitations of Coulomb scattering between 0D and 2D-confined quantum states. An experiment is designed which demonstrates the control of gain recovery for THz pulse trains in InGaAs QD-based SOAs under powerful electrical injection.

DOI: 10.1103/PhysRevLett.101.256803 PACS numbers: 78.67.Hc, 42.55.Px, 42.60.Da, 73.21.La

The understanding of the limiting mechanisms for the ultrafast gain recovery in InGaAs quantum dots (QDs) is the key for designing and engineering of high-speed performance of novel QD semiconductor optical amplifiers (SOAs). In particular, the mechanisms of gain buildup and its decay at very early time scales during the first few hundreds of femtoseconds is an intensively discussed problem in the current literature. Theoretical analyses cover a wide field of methods such as practical rate-equation approaches, extended numerical analysis of density matrices, and optical Bloch equations or microscopic scattering theories as well as a variety of combinations of them [1–8]. The investigation of the quantum memory of the quantum dot or 2D electron gas and its impact on linear spectra can be found in [4,5], or for electron gas dynamics in [9]. Experimental studies address the impact of p doping, wetting layer states, temperature, and intradot relaxation times (see, e.g., [10–14] and references therein). While QD applications like quantum computation require ultralong dephasing times and mechanisms which minimize any type of scattering events, the QD application for ultrafast pulse amplification might demand the opposite: extremely fast decay of coherence and efficient scattering to refill the QD states coupled to a reservoir of nonequilibrium charge carriers. Such a situation raises interesting future questions such as the size of the fundamentally shortest time scale for a scattering process, the chance of control of nonequilibrium population to design initial and final states for a scattering event, and the consequences for quantum dot level design by engineering QD and 2D-carrier system growth parameters.

In this Letter we investigate experimentally and theoretically the mechanisms of gain recovery and amplification of ultrafast pulse trains in InGaAs QDs and discuss ways of their control. An important goal is the more comprehensive understanding of the recently observed obstacle in amplification of femtosecond pulse trains with repetition frequencies f_{rep} above 200 GHz: As illustrated by the plot of the gain offset Δ in Fig. 1, the gain signal could not be completely switched back to its initial value with increasing f_{rep}, even for high injection currents I_{C}. In femtosecond heterodyne pump-probe experiments, we elucidate the potential of QD-SOAs for THz pulse train amplification under high carrier injection and driven at the optical amplification limit. The experimental findings are described by applying semiconductor quantum

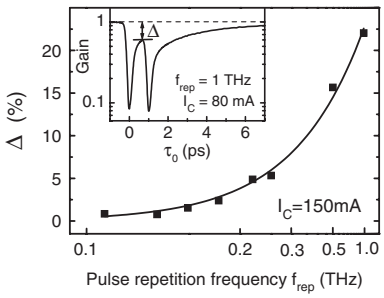

FIG. 1. Measured offset Δ for the QD-ground state as a function of temporal pulse separation of femtosecond double pulses at high electrical injection current $I_{\mathrm{C}} = 150$ mA. The gain reduction Δ is defined as shown in the inset for the example $I_{\mathrm{C}} = 80$ mA and $f_{\mathrm{rep}} = 1$ THz.

dot Bloch equations including microscopically calculated, temperature-dependent Coulomb scattering rates between quantum dot and 2D-continuum states.

A widespread intuitive assumption is that Coulomb scattering of QD states with a high density of energetically quasiresonant injected carriers in the 2D continuum of the wetting layer promotes an ultrafast gain recovery. An optimum adjustment of such scattering events needs the investigation of both electron and hole 0D-2D Coulomb in- and out-scattering rates $S_{\mathrm{in,out}}$ for a wide range of 2D-carrier densities and at elevated device temperature taking into account the carrier population functions. As a first step we calculate the scattering rates $S^b_{\mathrm{in,out}}$ with b denoting electron (e) or hole (h) states

$$S^b_{\mathrm{in,out}} = \frac{2\pi}{\hbar} \sum_{lmnb'} M_{nlmb}(2M^*_{nlmb} - \delta_{bb'} M_{lnmb}) f^{\mathrm{in/out}}_{lmnbb'} \delta(E^b + E^{b'}_n - E^b_l - E^{b'}_m)$$

with the energies E^b, E^b_l, $E^{b'}_m$, $E^{b'}_n$ and with $f^{in}_{lmnbb'} = \rho^b_l \rho^{b'}_m (1 - \rho^{b'}_n)$ and $f^{\mathrm{out}}_{lmnbb'} = (1 - \rho^b_n)(1 - \rho^{b'}_n)\rho^{b'}_n$ where ρ denotes the electron or the hole occupation probability within the 2D continuum. The scattering rates are determined by the Coulomb matrix elements M_{nlmb}. Our approach includes orthogonalized plane waves and goes beyond the Hartree-Fock approximation considering the Coulomb interaction up to the second order in the screened Coulomb potential (for details, see Refs. [3,7,8,15]). The sample temperature is implicitly included in the calculations by the temperature-dependence of the chemical potential $\mu(T)$ and of the screening function $\kappa(T)$. T influences essentially the statistics of the carrier population in the 2D continuum. This might crucially influence the density of available initial (final) states for a scattering event. As a first approach to analyzing dynamical experiments, we used in this Letter a kinetic description of the quantum dot amplifier dynamics: Scattering events between the quantum dot and the wetting layer are described within an energy conserving Born-Markov approximation which is valid for a significantly screened (high electron-hole densities), only weakly pump-pulse dependent Coulomb interaction in the 2D electron gas. In such an approximation the wetting layer can be treated as a bath. We argue that on the switching time scale (i) the pulse does not disturb the 2D electron gas too strongly, because it is off resonant and that (ii) the electron-transfer observation occurs beyond the time scale of the correlation time of the 2D electron bath, typically in the femtosecond range. With respect to these conditions, to similar results in Ref. [4], and justified by their success in comparison with the experimental results, a Markovian description is applied.

The results are plotted in Fig. 2(a) for electrons and Fig. 2(b) for holes. While for electrons S^e_{out} decays very rapidly with increasing n_{2D}, for holes the outscattering process becomes negligible only at a 2D-carrier density above 10×10^{12} cm^{-2}. A recently discussed question can

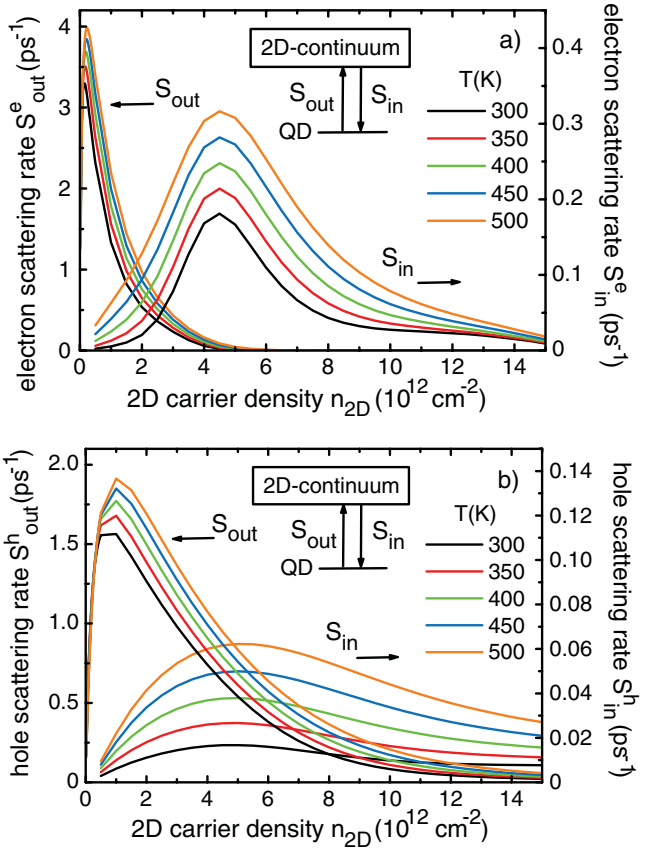

FIG. 2 (color). Temperature dependence of Coulomb scattering rates for (a) electrons and (b) holes. All rates first grow with the 2D-carrier density n_{2D} accounting for the increased number of available scattering partners. The rates decrease at high 2D densities due to the Pauli exclusion principle. The difference between electrons and holes can be traced back to their different effective mass. Both pure e-e (h-h) as well as mixed e-h (h-e) Coulomb scattering processes are included assuming $n^h_{2D} = 3.5 n^e_{2D}$ in agreement with the stationary values of the electron and hole 2D-carrier density [8].

be addressed by this calculation showing that an excess in hole 2D-carrier densities (e.g., by p doping) is supporting ultrafast refilling of the QD states. To significantly accelerate the Coulomb scattering process, a temperature increase of $\Delta T = 200$ K is necessary in theory which points to the fact that lattice temperature and charge carrier temperature are not in thermal equilibrium during the light-matter interaction (see below). The high injection current generates a hot 2D-carrier system in the wetting layer. At $n_{2D} = 6 \times 10^{12}$ cm^{-2}, the gain condition $S^e_{\mathrm{in}}(n_{2D}) T_{1,e}(n_{2D}) + S^h_{in}(n_{2D}) T_{1,h}(n_{2D}) > 1$ is fulfilled with $T_{1,e}$ and $T_{1,h}$ the microscopically determined electron and hole lifetimes [15]. We thus fix the parameter n_{2D} to this carrier density in our following calculations of the gain recovery dynamics.

The coupled polarization and occupation dynamics is determined by solving the resonant QD Bloch equations for the microscopic polarization p and populations f_e and f_h of electrons and holes [2]. The $T_{1,b}$ time with $b = e, h$ is

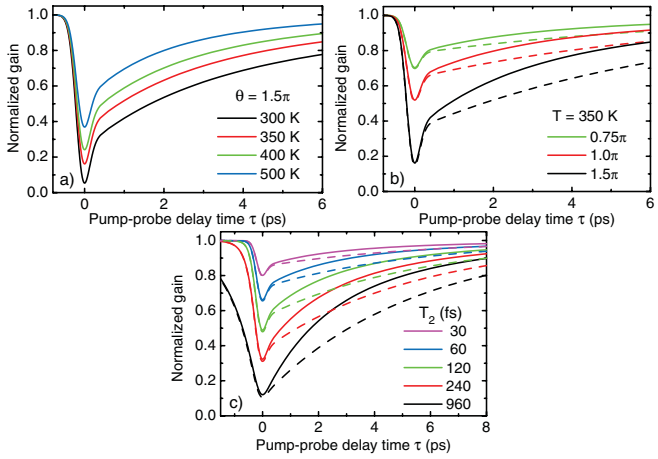

FIG. 3 (color). (a) Calculated gain vs time τ resonant to the QD ground state for different temperatures T at fixed $\theta = 1.5\pi$ for combined electron and hole Coulomb scattering. The T_2 times are 25, 20, 17, and 13 fs for $T = 300$, 350, 400, and 500 K, respectively. (b) Calculated gain vs τ for $\theta = 0.75$, 1.0, and 1.5π for a moderate $T = 350$ K, and $T_2 = 20$ fs. Dashed lines: only electron scattering rates. Solid lines: combined electron and hole scattering. (c) Calculation of the early gain dynamics at $\tau \sim 0$ with T_2 as parameter. The other parameters are $\theta = 0.5\pi$, $T = 400$ K. In all calculations the 2D-carrier density is $n_{2D} = 6 \times 10^{12}$ cm^{-2}, the input pulse intensity width is 150 fs and the QD dipole moment is set to $0.6e_0$ nm. The probe pulse is set to 0.01 of the pump-pulse field strength.

determined microscopically for each temperature and 2D-carrier density by $T_{1,b} = [S^b_{\text{in}} + S^b_{\text{out}}]^{-1}$ [3] while the dephasing time T_2 is calculated from electron-hole scattering (about 100 fs) and adjusted by an additional phenomenologically added value (for electron-phonon scattering [5]) accounting for the temperature increase by data from the experiment [16].

The results are plotted in Fig. 3 which shows the calculated normalized gain spectra in dependence of the pump-probe delay time τ for different temperatures T, pulse areas θ, and dephasing times T_2. Figure 3(a) shows the change in the gain recovery dynamics when the temperature T is increased accounting for a heated population in the 2D-carrier system. The gain recovery is, in particular, accelerated in the time range >1 ps, the time at which the scattering with the 2D continuum takes place as derived in Fig. 2. If the temperature gets too high, the more efficient scattering reduces on the one hand the gain recovery time, but acts also against the value of gain depletion at $\tau \sim 0$. Figure 3 also illustrates that at very early pump-probe delay times $\tau \sim 0$ a "coherent offset" is present in the dynamics indicating a coupled temporal development of polarization and population. Usually, such an early dynamics in gain recovery measurements is assigned to effects of two-photon absorption (TPA). Our calculations based on the semiconductor QD Bloch equations show that a "coherent offset" in the early gain dynamics can already be obtained without considering TPA. As can be seen from the calculations shown in Figs. 3(b) and 3(c), this "coherent offset" strongly depends on the optical pump-pulse area and the T_2 time of the investigated QD system. To achieve an extremely fast gain recovery immediately after the gain depletion, we obviously need to destroy the phase to leave the coherent regime and to bring the population back to the ground state. The short dephasing times used to qualitatively model the experiment point to the fact that phonon-induced dephasing [5] and heating [17] in quantum dot devices are of crucial importance for the understanding of ultrafast gain dynamics. For future analysis, an improvement in the theoretical description is possible by the incorporation of non-Markovian processes [5] in the scattering mechanisms and self-consistent combined non-thermal dynamics of electrons and phonons beyond the system-bath approximation [17].

From Fig. 3, we can finally also see that both electron and hole Coulomb scattering contribute to the fast gain recovery and have to be taken into account for device engineering, for example, for p-doping strategies.

Based on the gained theoretical insight we can, however, already now assign the optimum QD-sample parameter for high-frequency SOA operations: It should be a device with an active medium formed by InGaAs QD-in-a-well (DWELL) (introduces coupling to 2D-states due to quasiresonant energies) and a nominal p doping. The design should allow high electrical carrier injection and operation at I_C up to 200 mA. We investigate an InGaAs QD-SOA consisting of a deeply etched ridge waveguide of 2 μm width and 1 mm length with electrical contacts on top and bottom. The active medium is formed by 15 layers of MBE-grown InGaAs QD-in-a-well nanostructures with a nominal dot density of 2×10^{10} cm^{-2} and a nominal delta p doping of 5×10^{17} cm^{-3}. The amplified spontaneous emission (ASE) spectra for room temperature operation show two distinct peaks for the QD-ground (excited) state excitonic emission at 1.285 μm (1.2 μm). The SOA-device temperature is derived from the temperature evolution of the phase shifts in the waveguide resonator modes using high-resolution spectra of the ASE. With increasing I_C from 8 to 150 mA the device temperature increases from room temperature by $\Delta T_{\text{device}} = 73$ K with a slope of 0.52 grad/mA (35 mA $< I_C <$ 150 mA). This confirms the necessity to take into account heating effects in the 2D continuum in the numerical analysis.

The optical pump and probe pulses are generated by an optical parametric oscillator pumped by a high-repetition Ti:sapphire laser. Using two Michelson interferometers, up to four 150 fs long Fourier-limited pump pulses of $\sim$0.1 pJ are generated with a delay τ_0 between 0.5 ps $< \tau_0 <$ 10 ps corresponding to pulse repetition frequencies of 2 THz $< f_{\text{rep}} <$ 100 GHz. The intensity ratio between optical pump and probe pulse is set to $I_{\text{probe}}/I_{\text{pump}} = 0.01$. In Fig. 4(a) we show exemplarily the amplification of a femtosecond four-pulse train of 1 THz repetition frequency [18]. Figure 4(b) shows the change in the gain at the two selected times $\tau = 0$ and $\tau = 5$ ps. With increasing injection cur-

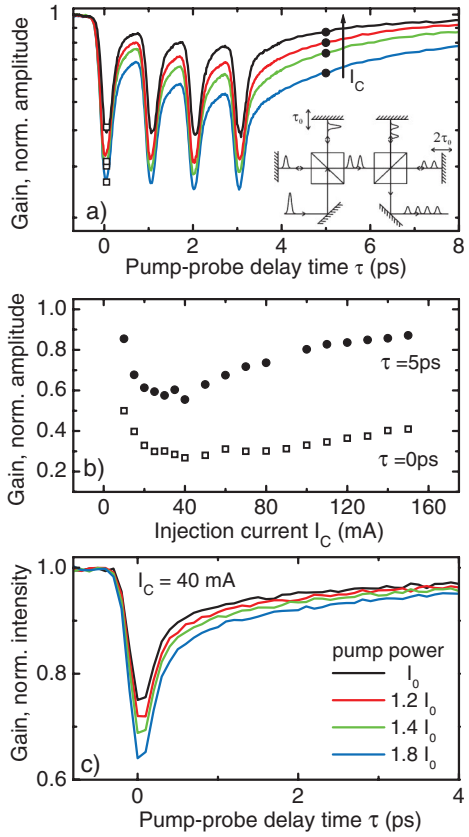

FIG. 4 (color). (a) Normalized gain as a function of τ for increasing $I_C = 50$ mA (blue or dark gray), 80 mA (green or light gray), 100 mA (red or gray), 150 mA (black). The four-pulse THz pump-pulse train is generated by a two-stage Michelson interferometer as shown in the inset. (b) I_C dependence of the first gain peak at $\tau = 0$ ps (squares) and of the gain at fixed delay $\tau = 5$ ps (circles) after a four-pulse THz pulse train. (c) Optical pump power dependence of the very early gain dynamics around $\tau \sim 0$ measured for a single pulse at fixed $I_C = 40$ mA.

rent we can clearly control the gain recovery offset after the pulse train passed the sample. Also the absolute gain depletion at $\tau = 0$ varies with I_C [Fig. 4(b)] and optical pump power [Fig. 4(c)]. The gain offset can be minimized almost up to its initial value if we apply the highest $I_C = 150$ mA [Fig. 4(b)]. In agreement with our discussion above, a variation of the current I_C in the experiment can obviously be qualitatively modeled by a variation of 2D-carrier density and temperature in theory. A single pulse experiment at a fixed injection current shows the behavior predicted in Fig. 3(b), i.e., for fixed I_C the gain depletion is increased if the pump-pulse intensity grows. Finally, we found a slowing down of the gain recovery dynamics if we vary the SOA temperature by external cooling, but constant injection current of $I_C = 40$ mA (not shown), which we can preliminarily assign to a modification in coupling to phonons and thus a modification in T_2 or modifications of the occupations f_e and f_h as discussed in Fig. 3.

In conclusion, we found that phonon-induced dephasing and a heated carrier population in the 2D continuum are crucial for the QD-gain recovery. To model the ultrafast gain dynamics, very short dephasing times $T_2 < 100$ fs and Coulomb scattering rates at elevated temperatures up to $T = 500$ K need to be considered. The initial subpicosecond dynamics is governed by the optical pump-pulse area and small T_2 times as well. For a fixed 2D-carrier density, e.g., here $n_{2D} = 6 \times 10^{12}$ cm^{-2}, remarkable Coulomb inscattering rates from the 2D continuum in the QD bound states are found with ~ 0.3 ps^{-1} for electrons and ~ 0.06 ps^{-1} for holes at $T = 500$ K. Experimentally the gain recovery time is substantially accelerated in QD-DWELL structures at injection currents >80 mA.

We acknowledge financial support by SFB 787 and the NoE SANDiE.

*ulrike.woggon@tu-berlin.de

[1] M. Sugawara *et al.*, Phys. Rev. B **69**, 235332 (2004).
[2] H. C. Schneider W. W. Chow, and S. W. Koch, Phys. Rev. B **64**, 115315 (2001); W. W. Chow and S. W. Koch, IEEE J. Quantum Electron. **41**, 495 (2005).
[3] T. R. Nielsen P. Gartner, and F. Jahnke, Phys. Rev. B **69**, 235314 (2004).
[4] H. C. Schneider W. W. Chow, and S. W. Koch, Phys. Rev. B **70**, 235308 (2004).
[5] M. Lorke *et al.*, Phys. Rev. B **73**, 085324 (2006).
[6] D. Deppe and H. Huang, IEEE J. Quantum Electron. **42**, 324 (2006).
[7] E. Malic *et al.*, IEEE J. Sel. Top. Quantum Electron. **13**, 1242 (2007).
[8] K. Lüdge *et al.*, Phys. Rev. B **78**, 035316 (2008).
[9] H. Haug and A. P. Jauho, *Quantum Kinetics in Transport and Optics of Semiconductors* (Springer, New York, 2007).
[10] J. Urayama *et al.*, Phys. Rev. Lett. **86**, 4930 (2001).
[11] D. R. Matthews *et al.*, Appl. Phys. Lett. **81**, 4904 (2002).
[12] T. Markussen *et al.*, Phys. Rev. B **74**, 195342 (2006).
[13] S. Dommers *et al.*, Appl. Phys. Lett. **90**, 033508 (2007).
[14] V. Cesari *et al.*, Appl. Phys. Lett. **90**, 201103 (2007).
[15] E. Malic *et al.*, Appl. Phys. Lett. **89**, 101107 (2006).
[16] P. Borri *et al.*, IEEE J. Sel. Top. Quantum Electron. **8**, 984 (2002).
[17] S. Butscher *et al.*, Appl. Phys. Lett. **91**, 203103 (2007).
[18] The plotted gain is normalized to 1.0 for a better discussion of theory and experiment. For comparison, the absolute peak gain values $G(\tau = 0)$ obtained for the measured SOA device vary between -12 dB achieved at $I_C = 60$ mA and -8 dB at $I_C = 15$ mA. The theoretical gain is calculated according to $g(\omega, \tau) \propto -\omega \mathrm{Im}\{[P_{\mathrm{pump+probe}}(\omega, \tau) - P_{\mathrm{pump}}(\omega)]/E_{\mathrm{probe}}(\omega)]\}$ for $\omega = \omega_{\mathrm{gap}}$.